Available online at www.sciencedirect.com

SciVerse ScienceDirect

Ceramics International 38 (2012) 6795–6805

CERAMICS INTERNATIONAL

www.elsevier.com/locate/ceramint

Kinetics of growth of superhard boride layers during solid state diffusion of boron into titanium

B. Sarma*, N.M. Tikekar, K.S. Ravi Chandran

Department of Metallurgical Engineering, 135 South 1460 East Room 412, The University of Utah, Salt Lake City, UT 84112, USA

Received 1 February 2012; received in revised form 17 April 2012; accepted 23 May 2012
Available online 15 June 2012

Abstract

Solid state boriding of titanium is a very effective and inexpensive way to create surface layers that can impart high hardness and wear resistance. In this work, the growth kinetics of hard titanium boride layers created by the solid-state boron (B) diffusion through titanium (Ti) surface at various temperatures has been determined. The hard boride layers comprised of a monolithic titanium diboride (TiB_2) layer at the top and a titanium boride (TiB) sub-layer that mostly consisted of TiB whiskers with high aspect-ratio growing normal to the surface. The structure and the crystallography of the layers were also confirmed by X-ray diffraction. Experimental results show that the growth rates of the TiB_2 as well as the composite (TiB_2+TiB) coating layers follow the parabolic kinetics. It is shown that the thickness development as a function of time can be predicted reasonably accurately, using the error function solutions for the two simultaneously growing boride layers developed in our previous work. The maximum degree of growth as dictated by the diffusivity of B in the boride phases was achieved using a solid state B powder pack in an ambient furnace atmosphere.

Keywords: Titanium boride; Diffusion; Whiskers; Kinetics

1. Introduction

It is well known that titanium (Ti) in heavy duty tribological and contact conditions suffers from high volumetric wear, galling, and seizure of surfaces. To mitigate these, surface hardening techniques such as the nitriding [1,2] or oxidizing [3–5] of titanium surfaces were pursued. A good review of the developments until the 1990s can be found in Ref. [5]. Nitriding increases the surface hardness of Ti to about 9–12 GPa (Vicker's hardness (Hv)) [6,7] with a moderate increase in wear resistance [8,9]. This is attributed to the dispersion of TiN and Ti_2N phases in the subsurface region to a depth of about 10–25 μm. In oxygen-based surface hardening, oxygen enrichment leads to a surface hardness of about 5–12 GPa Hv [10,11], and has been found to improve the abrasive wear and/or scratch resistance. However, the use of these hardening techniques is limited for various reasons. This is partly due to the fact that the surface hardness levels attainable by nitriding or oxidizing are, at best, about 10–12 GPa which is comparable to that obtained in surface hardened steels or unhardened tool steels. Additional issues such as the poor underlying support of the substrate beneath the titanium nitride layers [9] and the possible embrittlement of titanium substrate due to the presence of nitrogen or oxygen as interstitials also pose some intrinsic limitations.

Borides of titanium have a much higher hardness and wear resistance [12,13]. In our past research [14–16] the feasibility of solid state diffusion of boron into titanium to create hard (>15 GPa) and wear resistant surface layers up to depths of about 50 μm was demonstrated. The diffusion leads to two layers of borides, with the top layer being titanium diboride (TiB_2) and the second layer being titanium boride (TiB). The TiB_2 grows as solid monolithic layer while the TiB below it predominantly grows as pristine whiskers, generally perpendicular to the surface. These hard dual layers provide a unique surface-modified structure that builds high surface hardness and wear resistance—the TiB_2 layer provides surface hardness levels in excess of 30 GPa Hv and the TiB whiskers, in addition

*Corresponding author. Tel.: +1 801 682 0619.
E-mail address: biplabsarma@gmail.com (B. Sarma).

0272-8842/$36.00
http://dx.doi.org/10.1016/j.ceramint.2012.05.077

to having high hardness (> 15 GPa Hv), anchor the coating into the substrate, which is very desirable for coating durability. In fact, it has been shown recently [17,18] that 6.35 mm dia. Ti balls borided with such a dual layer coating (for ball bearings) have superior wear resistance (about 40 × better) than fully alumina balls when abraded against alumina disk.

There are a few studies of boride layer growth on titanium [13,19–22], but none address the detailed kinetics and explain the growth mechanisms. The earliest work in the area of titanium boriding was performed by Krzyminski and Kunst [13] and Chatterjee-Fischer and Schaaber [19]. These studies showed that boride layer growth by the diffusion from solid B media is possible when boriding is performed in a controlled atmosphere with a reduced oxygen partial pressure. A more recent work [21] also confirmed the key finding of Krzyminski and Kunst that at a reduced oxygen partial pressure (1 Pa), the reaction activity is the highest for boriding.

The primary objective of this work is to fully establish the kinetics of the growth of titanium boride layers as a function of boriding temperature in the α and β phase fields of Ti. The structure and the growth kinetics of the boride layers formed at temperatures above and below the beta transus (β-transus) temperature of Ti and the mathematical framework to predict the kinetics are very important both from fundamental and application points of view. More importantly, the emphasis of this study is on solid state boron diffusion process in *a* regular furnace atmosphere as opposed to the controlled atmosphere that was used in the studies mentioned above. The additional objective is to show that error function solutions based on Fick's second law, developed for the two simultaneously growing layers, predict the layer growth kinetics quite well.

2. Experimental procedure

Commercially pure titanium (CP-Ti, Grade 2, composition in wt%:0.3 Fe, 0.25 O, 0.1 C, 0.03 N, 0.015 H and 0.3 max. of other elements) samples (30 mm × 14 mm × 6 mm) were polished to 800 grit surface finish. A boriding powder mixture comprising a B source (amorphous boron, Composition in wt%: 95–97 B, 0.89 Mg, 0.12 water soluble B, particle size FN 0.694, from SB Boron Corporation, Bellwood, IL), a transport medium (99% pure anhydrous sodium tetraborate from Alfa Aesar Inc.) and carbon activator (99.5% pure from Alfa Aesar Inc.) was prepared by ball milling the powders for about 16 h. The mixture was tightly packed in a crucible ensuring a sufficiently thick (> 1'') pack all around the sample. Boron diffusion experiments were conducted by heating (rate: 10 °C/min) the pack to temperatures in the range 850–1050 °C for periods up to 24 h in an ambient furnace atmosphere. After the treatment, the formation of different phases on the borided samples was identified using SIEMENS D5000 diffractometer with copper K_α radiation. The diffraction tests were done by θ to θ scan from 20° to 100°. The samples were then sectioned, metallographically polished and etched. Boride layer structure was examined using scanning electron microscopy (SEM). Thicknesses of TiB_2 layer and the composite (TiB_2+TiB whisker) coating layer

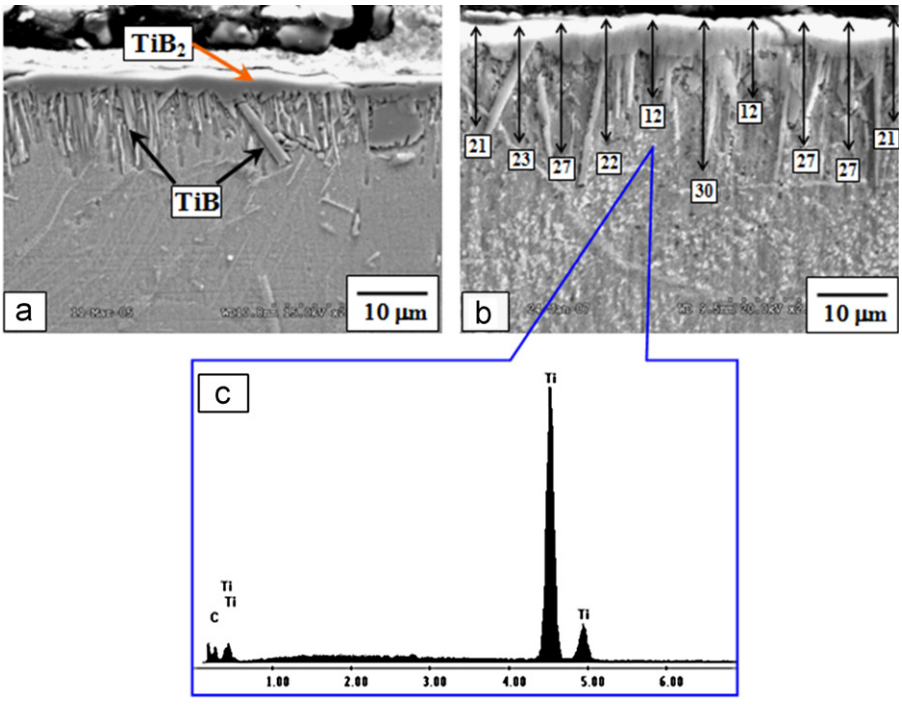

Fig. 1. SEM micrographs of coating structure in CP-Ti borided at 850 °C for (a) 3 h and (d) 24 h, the vertical arrows in (b) and the numbers in boxes indicate the total coating thickness at equally spaced locations (c) the EDX profile of the Ti substrate in between TiB whiskers.

were determined from SEM micrographs on the basis of averages of measurements at ten equally spaced locations, as illustrated in Fig. 1(b). This involved measuring the distance of the farthest location of the tip of the intercepted TiB whisker, from the specimen edge, at ten equally spaced locations. For each boriding condition, such measurements were made on three different micrographs and the averages and the standard deviations of these measurements were determined. The TiB_2 grew as a continuous monolithic layer—its thickness could be readily measured at ten equally spaced locations on multiple SEM micrographs.

3. Results and discussion

3.1. Structure of boride layers

The average coating thicknesses and standard deviations for the TiB_2 and the composite (TiB_2+TiB) coating layers are given in Table 1 for different treatment temperatures and times. Microstructures of the dual layer coatings obtained after boriding at 850 °C for 3 h and 24 h are shown in Fig. 1(a and b). A continuous and thin outer layer of TiB_2, followed by TiB whiskers penetrating normally into the substrate can be seen. Even though the outer TiB_2 layer constituted only a small fraction of the total coating thickness (Table 1), it was almost completely continuous in all the treatments. The thickness of the TiB_2 layer increased from 1.5 μm at 3 h to 3.9 μm at 24 h. The TiB layer is made of extremely fine TiB whiskers that have needle-like morphology with thicknesses in the range of 10–100 nm. The presence of some isolated ends of TiB whiskers located far inside the substrate can be seen in the 3 h treatment (Fig. 1a)—these seem to be the ends of TiB whiskers that originated from somewhere behind the plane of polishing. The outlines of TiB whiskers were found to be quite well defined and they were found to be thicker after longer treatment times compared to that seen in shorter treatment times. It is evident from the micrographs that, like TiB_2, the TiB phase does not grow as a monolithic layer. Hence, when we refer to the "TiB layer" it is implied that it is a layer of TiB whiskers with Ti located in between. The EDX profile of the substrate in between the TiB whiskers confirms the presence of Ti only as shown in Fig. 1c.

The structures of boride layers after 950 °C treatment for 3 h and 24 h are shown in Fig. 2(a and b). A continuous TiB_2 layer followed by TiB whiskers penetrating into the CP-Ti substrate, similar to that at 850 °C, can be seen. The TiB_2 layer is slightly thicker and the TiB whiskers seem to penetrate deeper into the substrate, compared to that at 850 °C. Both the TiB_2 and TiB layer thicknesses increased by a factor ≥ 2, on going from 3 to 24 h. Micrographs of samples borided at 1050 °C (this temperature is well into the β-phase field of titanium) for 3 h and 24 h are presented in Fig. 3(a and b). Due to the high temperature diffusion treatment, a thicker TiB_2 layer

Table 1
Averages thickness values of TiB_2, TiB and the composite (TiB_2+TiB) coating layers, determined for different B diffusion temperatures and times.

Time (h)	850 °C			950 °C			1050 °C		
	TiB* (μm)	TiB_2 (μm)	Total (μm)	TiB (μm)	TiB_2 (μm)	Total (μm)	TiB (μm)	TiB_2 (μm)	Total (μm)
0.083	13	0.5 ± 0.1	13.5 ± 3.0	15	1 ± 0.1	16 ± 2.5	15	1.5 ± 0.1	16.5 ± 1.9
3	21.5	1.5 ± 0.1	23 ± 3.2	22.8	3.2 ± 0.3	26 ± 2.7	26	5 ± 0.3	31 ± 2.5
6	21.3	2.7 ± 0.2	24 ± 3.5	24.2	4.8 ± 0.2	29 ± 3.2	27	10 ± 0.7	37 ± 3.4
12	21.8	3.2 ± 0.2	25 ± 4.2	28.6	5.4 ± 0.3	34 ± 3.3	29	12 ± 0.9	41 ± 3.6
18	22.7	3.3 ± 0.3	26 ± 5.4	39.3	5.7 ± 0.3	45 ± 4.4	35	15 ± 0.9	50 ± 5.7
24	24.1	3.9 ± 0.3	28 ± 6.3	40.6	6.4 ± 0.4	47 ± 5.4	37	17 ± 1.0	54 ± 5.9

*TiB coating thickness was determined by subtracting the average thickness of TiB_2 layer from the average total coating thickness, hence there is no S.D. for these data.

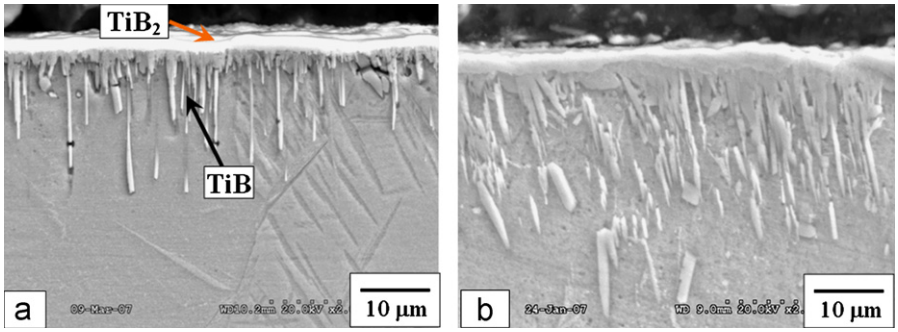

Fig. 2. SEM micrographs of coating structure in CP-Ti borided at 950 °C for (a) 3 h, and (b) 24 h.

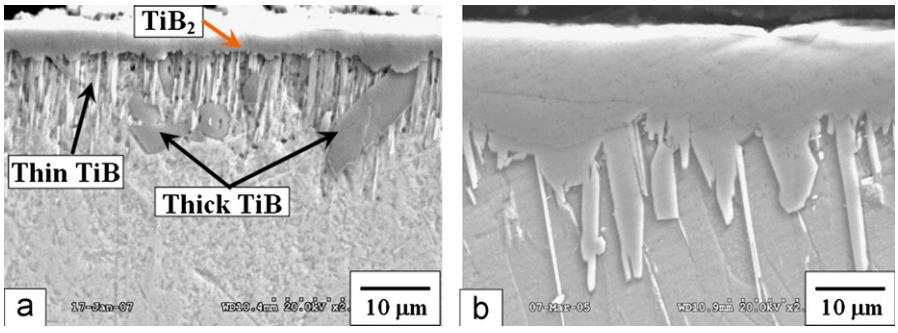

Fig. 3. SEM micrographs of coating structure in CP-Ti borided at 1050 °C for (a) 3 h, and (d) 24 hr.

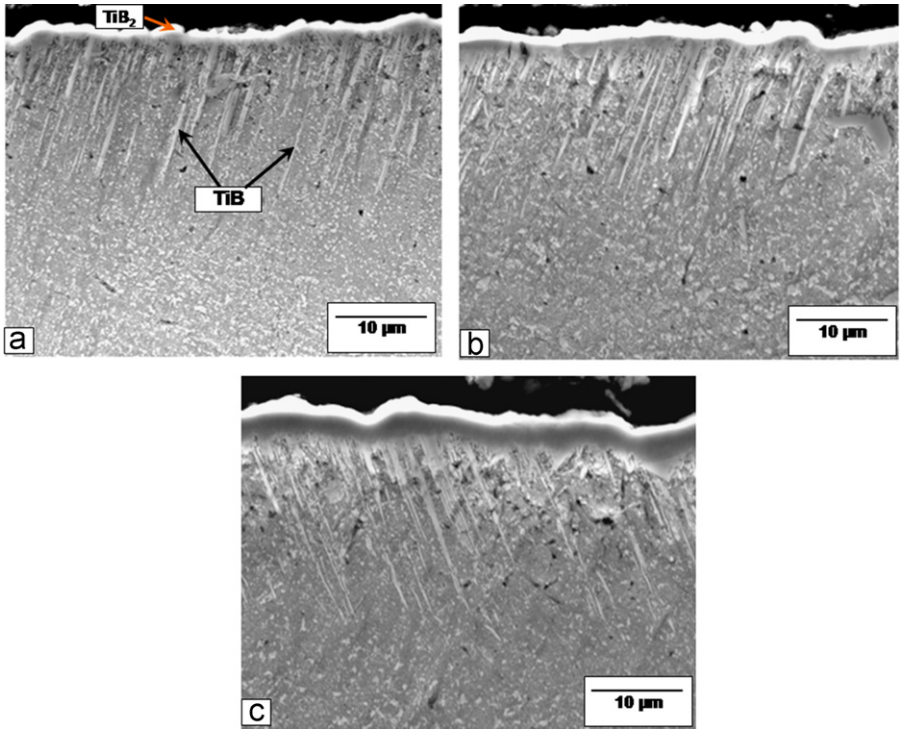

Fig. 4. SEM micrographs of CP-Ti samples borided for 5 min at different temperatures (a) 850 °C, (b) 950 °C and (c) 1050 °C.

was observed in all the samples. The TiB_2 thickness increased by a factor of 3 from 5 μm at 3 h to 17 μm at 24 h. (Table 1) indicating that the growth rate of TiB_2 layer is relatively faster than that observed at 850 and 950 °C. Unlike the TiB whisker structure at 850 °C, the TiB whisker layer at 1050 °C seems to be actually made of two size groups: the individual nano-sized whiskers and a much thicker micron-sized TiB phases (Fig. 3a and b).

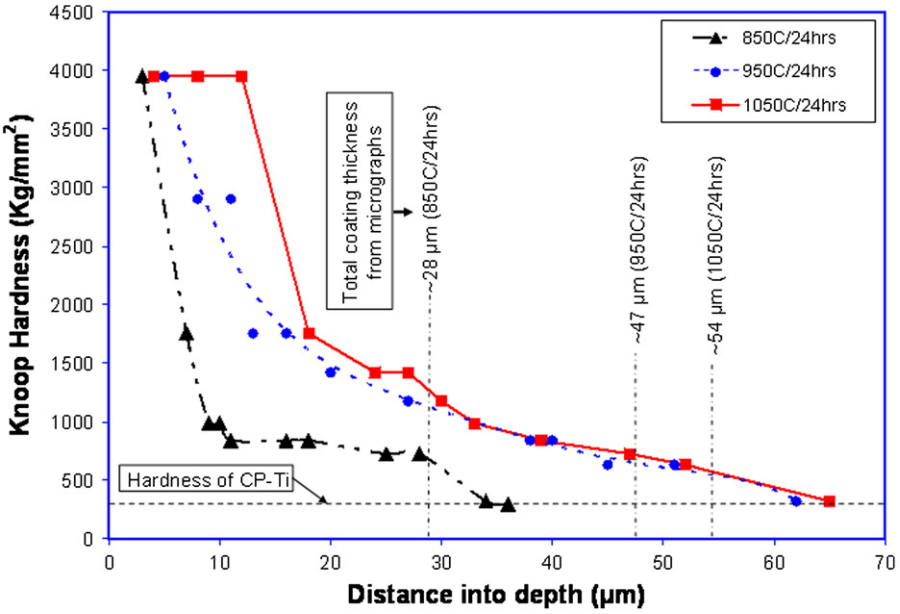

Fig. 5. Knoop hardness profile of the (TiB_2+TiB) boride layer formed at 850 C, 950 C and 1050 C after 24 h of diffusion treatment time. The hardness of CP-Ti (~300 kg/mm^2) is also shown for reference.

Nevertheless, the depth to which the TiB whiskers penetrated into the substrate increased with time.

The SEM micrographs of samples borided for 5 min at 850 °C, 950 °C and 1050 °C are shown in Fig. 4(a–c), respectively. Three important observations can be made from these micrographs and the data in Table 1, with respect to the nature of growth of individual layers and their relative dominance. First, based on the short term (5 min/0.083 h) layer thickness data, it is clear that a substantial growth of TiB whiskers occurs very early—it is likely that TiB formation actually started at relatively low temperatures, and that some pre-grown TiB existed even before reaching the isothermal treatment temperatures. This is evident from the fact that at 850 °C, the TiB growth after 5 min (13 μm) is more than that occurred between 3 h to 24 h (3 μm). Second observation is that there is not much growth of TiB_2 during the short term (5 min) diffusion—most of the TiB_2 growth actually occurred during the isothermal hold periods at the diffusion temperatures. Third observation is that the change in the TiB whisker layer thickness, on going from 5 min to 24 h diffusion, reaches a maximum at 950 °C—the changes in the TiB whisker layer thickness are ~11 μm, 25 μm and 22 μm for 850 °C, 950 °C and 1050 °C, respectively. Thus, it is clear that most of the increase in the total coating thickness is due to the increased contribution of TiB whisker layer at 950 °C and that of TiB_2 layer at 1050 °C. The rates of growth of TiB_2 and the composite (TiB_2+TiB) coating layers were found to follow the parabolic growth kinetics, but they were dependent on whether the treatment temperature was in α-field or β-field or proximal to the β-transus—a more detailed account of the effects during diffusion near β-transus are presented elsewhere [23].

Knoop hardness profiles across the boride layers in samples borided at 850 °C, 950 °C and 1050 °C after 24 h of treatment times are shown in Fig. 5. The surface layers are hardened to a depth of about 30 μm in 850 °C/24 h sample and to about 60 μm in both 950 °C/24 h and 1050 °C/24 h samples, which are consistent with the SEM observations of the coating depths. The hardening depth is slightly higher than the actual depth of the layer despite the fact that the coating depth in the micrograph was measured as the farthest tip of the growing TiB whiskers. This suggests that the thickness measurements from the micrographs can be taken as the conservative coating thickness values and can be used for comparison with theory. The high hardness (> 3000 kg/mm^2) region near the surface corresponds to the thin layer of TiB_2. The subsurface boride layer is actually a mixture of TiB whiskers and TiB_2 monolith, or the transition region, which explains the steep decrease in hardness with distance in to the substrate. The hardness of monolithic TiB is about 2000 kg/mm^2. The coating structures beyond the TiB_2 are a mixture of TiB and Ti, with the volume fraction of TiB gradually decreasing with distance into the depth. The decreasing hardness profile in this region is consistent with the variations in TiB/Ti phase proportions in the sublayer.

The X-ray diffraction patterns for the boride layers are given in Fig. 6(a and b) for the 3 h and 24 h diffusion treatments at various temperatures. It can be observed that the borided layers consisted mostly of TiB_2 and TiB compounds, with a clear dominance of TiB_2 phase in the 1050 °C treatments. However, for 3 h, the 850 °C and the 950 °C treatments showed relatively higher concentrations of TiB whiskers. In particular, for the 24 h treatment, a relatively high concentration of TiB was found at 950 °C,

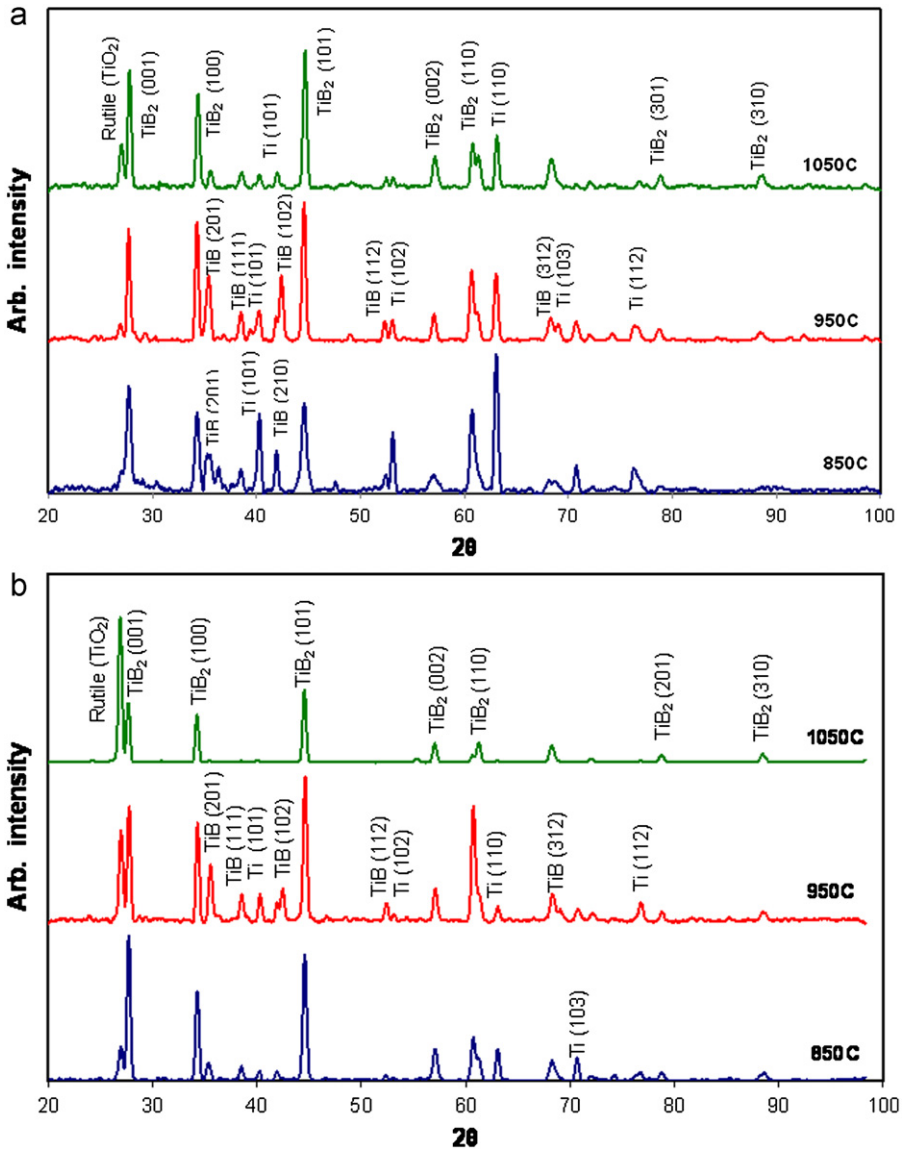

Fig. 6. X-ray diffraction profiles for the coatings borided at different temperatures for (a) 3 h and (b) 24 h.

Table 2
Diffusivity data [29] used in the calculations of kinetics using error function solutions.

T (°C)	Chemical diffusivity of B in TiB_2 (m^2/s)	Chemical diffusivity of B in TiB (m^2/s)
850	1.34×10^{-16}	6.13×10^{-15}
950	6.92×10^{-6}	3.25×10^{-14}
1050	2.78×10^{-15}	1.34×10^{-13}

compared to the other two temperatures. These observations are consistent with the SEM microstructures, in that, the 950 °C/24 h condition resulted in the highest TiB layer thickness. As reported in a recent study [21], the X-ray diffraction patterns also indicate the presence of rutile titanium oxide (TiO_2) in the surface of all borided samples. However, the presence of this oxide layer could not be detected by SEM as the thickness of this layer is apparently very small. It is to be noted that only one peak in the diffraction patterns could be assigned to TiO_2. There was no evidence of oxide phase within the boride layers. It is possible that the oxide layer had formed when the crucible was removed from the furnace after cooling to 500 °C after boriding. Further, as will be evident in the next section, the oxide layer does not appear to have influenced the growth kinetics.

3.2. Modeling of layer growth kinetics

Prior work on quantitative prediction of the growth of boride layers on Ti is quite limited. For the growth of multiple compound layers by diffusion, error-function based solutions [24,25] of Fick's second law can be used to predict the kinetics. The growth of FeB/Fe_2B layers on Fe during boriding is somewhat similar to the growth of boride layers here. The kinetics of growth of FeB/Fe_2B

layers have been predicted using the diffusivity of B alone [26–28] and assuming that the diffusion of metal component is negligible. In the present analysis, the chemical diffusivity values of B in TiB_2 and TiB (determined from the work of Fan et. al. [29]) were used (Table 2) to predict the growth of the two boride layers. In the Ti–B system, TiB_2 is a stoichiometric line compound and TiB has narrow stoichiometric range. Thus, in practice, diffusional growth of these compounds under B concentration gradient does not involve large concentration gradient within the phases. Nevertheless, the concentration difference between $B/TiB_2/TiB$ layers can be considered to represent the average compositional gradients in the phases.

In our recent publication [23], an effort was made to model the growth kinetics of boride layers on Ti using error function approach. However, the modeling aspects were pertaining to growth of layers at temperature close to the α/β phase transition temperature in Ti (910 °C). As elucidated in the article, the growth behaviors of the layers near the transition temperature are quite different compared to when B diffusion experiments are performed away from it (in complete α and β phase fields). Here, with the experimental results of boride layers at temperatures 850, 950 and 1050 °C, we would examine whether a similar theoretical model can also describe the growth kinetics of these layers at these temperatures. The detailed modeling procedure was explained in Ref. [23], however, the fundamental aspects as well as some key equations of the model are discussed in the following.

The development of the error function solutions will be illustrated on the basis of growth of TiB_2/TiB whisker layer on titanium (Fig. 7(a)). Three interfaces exist in this system: the B–TiB_2 interface, TiB_2–TiB interface and the TiB–Ti interface. The B concentration profiles across the layers are schematically shown in Fig. 7(b). The Fick's second law of diffusion, relating the changes in concentration of B with time and location is:

$$\frac{\partial C}{\partial t} = D\frac{\partial^2 C}{\partial x^2} \tag{1}$$

where D is the diffusion coefficient and C is the concentration. The development of error function solutions is based on the following assumptions: (i) the growth of the dual layer is controlled only by the diffusion of B and the diffusion of Ti in the opposite direction can be ignored [29], (ii) the diffusion coefficient of B is concentration independent, and (iii) the solubility of B in Ti-matrix is negligible [30]. The aforementioned assumptions are based on the prior works as described in Ref. [29]. It was suggested that the growth of the TiB_2 and the TiB are limited only by the sluggish diffusion of B through these layers. The kinetics of the interfacial reactions is much faster compared to that of the B diffusivities through these layers. On the other hand, the diffusivities of Ti in these phases are couple of orders of magnitude lower than that of B as it diffuses substitutionally. Hence, from the modeling perspective, the influence of Ti diffusion on the boride layer growth can be neglected. The homogeneity range of the TiB_2 and the TiB layers are rather small (~1 at%) and are considered line compounds for all practical purposes. Therefore, it is reasonable to assume that the diffusion coefficient of B is independent of the concentrations in these layers.

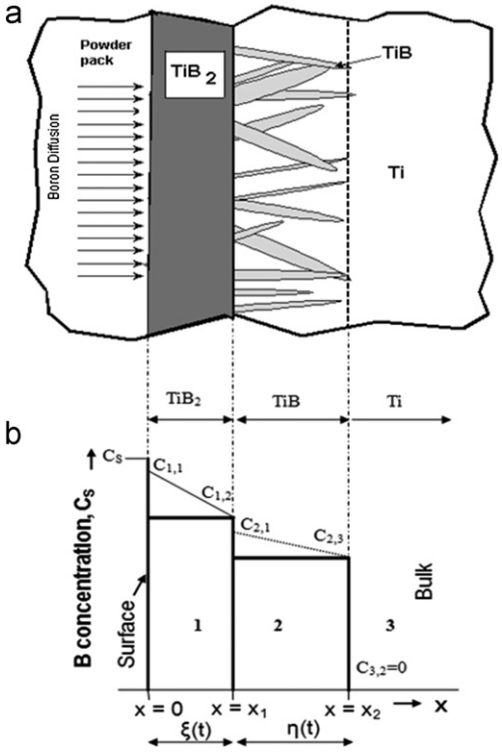

Fig. 7. (a) Schematic of growth of the TiB_2 layer and the TiB whisker layer (b) concentrationprofile of B across the layers.

With these assumptions, the initial and boundary conditions can be written as:

Initial conditions: ($t=0$).

The effective weight fraction of B in the powder mixture is C_S, hence,[1]

$$C = C_S = 054 \text{ at } x = 0 \tag{2}$$

$$C \text{ (in } TiB_2/TiB) = 0 \text{ for } x > 0 \tag{3}$$

Boundary conditions: ($t > 0$).

$$C = C_{1,1} = \text{upper limit of B concentration in } TiB_2 = 0.311 \tag{4}$$

$$C = C_{1,2} = \text{lower limit of B concentration in } TiB_2 = 0.301 \tag{5}$$

$$C = C_{2,1} = \text{upper limit of B concentration in TiB} = 0.185 \tag{6}$$

[1] In this model calculation, the B concentrations are taken as weight fractions in all phases. To maintain this consistency, the value of the surface B concentration (C_S) was also considered in weight fraction of the powder mixture. Note that the powder mixture consists of a boron source, a transport medium and an activator.

$$C = C_{2,3} = \text{lower limit of B concentration in TiB} = 0.18 \tag{7}$$

$$C = C_{3,2} = \text{B concentration in Ti matrix} = 0 \tag{8}$$

The general solutions for B concentration in the boride layers and for that in Ti matrix which satisfy Eq. (1) are of the form [24,25]:

$$C_i(x,t) = A_i + B_i \ \text{erf}\left(\frac{x}{2\sqrt{D_i t}}\right) \tag{9}$$

where C_i and $D_i$are the concentration and diffusivity of B in the respective phase (TiB_2, TiB or Ti). A_i and B_i are the respective constants for each phase which need to be determined from the initial and boundary conditions. From Fig. 7(b), defining the time-independent interface boundary positions for TiB_2 and TiB in terms of dimensionless growth-rate parameters ξ and η, respectively, one can write [24]:

$$x_1 = 2\xi\sqrt{D_1 t} \tag{10}$$

$$x_2 = 2\eta\sqrt{D_2 t} \tag{11}$$

where x_1 and $x_2$are the positions of TiB_2/TiB and TiB/Ti interface boundaries, respectively. D_1 and $D_2$are the respective diffusion coefficients of B in TiB_2 and TiB phases. Using Eqs. (10) and (11) and incorporating the initial and boundary conditions [(Eqs. (2)–(8) in Eq. (9)], the variations of concentrations of B in TiB_2 and TiB phases are given by:

$$C_{TiB_2}(x,t) = C_S - \left(\frac{C_S - C_{1,2}}{\text{erf}\,\xi}\right)\text{erf}\left(\frac{x}{2\sqrt{D_1 t}}\right) \tag{12}$$

$$C_{TiB}(x,t) = C_{2,1} - (C_{2,1} - C_{2,3})\left(\frac{\text{erf}\left(\frac{x}{2\sqrt{D_2 t}}\right) - \text{erf}(\phi\xi)}{\text{erf}\,\eta - \text{erf}(\phi\xi)}\right) \tag{13}$$

where $\phi = \sqrt{\frac{D_1}{D_2}}$

During the growth of the layers, simultaneous advancement of the TiB_2/TiB and TiB/Ti interface boundaries at x_1 and x_2 in a small time step (dt) will occur because of the accumulation of B atoms at those interfaces driven by the differences in B flux between TiB_2, TiB and Ti phases. Hence, applying the rule of mass conservation at the TiB_2/TiB and TiB/Ti interfaces, one can write [23]:

$$(C_{1,2} - C_{2,1})\left(\frac{dx_1}{dt}\right) = -D_1\left(\frac{\partial C_{TiB_2}}{\partial x}\right)_{x=x_1} + D_2\left(\frac{\partial C_{TiB}}{\partial x}\right)_{x=x_1} \tag{14}$$

$$(C_{2,3} - C_{3,2})\left(\frac{dx_2}{dt}\right) = -D_2\left(\frac{\partial C_{TiB}}{\partial x}\right)_{x=x_2} \tag{15}$$

Differentiating Eqs. (10), (12), and (13) and incorporating in Eq. (14) yields:

$$\left(\frac{C_S - C_{1,2}}{\xi\sqrt{\pi}\,\text{erf}\,\xi}\right)\exp(-\xi^2) - \frac{(C_{2,1} - C_{2,3})}{\xi\varphi\sqrt{\pi}(\text{erf}\,\eta - \text{erf}(\phi\xi))}\exp(-\phi^2\xi^2) = (C_{1,2} - C_{2,1}) \tag{16}$$

Similarly, differentiating Eqs. (11) and (13) and incorporating in Eq. (15) yields:

$$\frac{(C_{2,1} - C_{2,3})}{\eta\sqrt{\pi}(\text{erf}\,\eta - \text{erf}(\phi\xi))}\exp(-\eta^2) = (C_{2,3} - C_{3,2}) \tag{17}$$

Eqs. (16) and (17) are non-linear and are to be solved for two unknown parameters, ξ and η, which are the growth parameters for the TiB_2 and TiB layer, respectively. These equations were solved simultaneously using MATLAB program and ξ and η were determined for the three treatment temperatures (850 °C, 950 °C and 1050 °C). From the growth parameters, the time-dependent layer thicknesses for the TiB_2 and TiB layers can be calculated using Eqs. (10) and (11), respectively.

An important aspect needs to be considered in comparing the predicted growth rates of the TiB_2 and TiB layers with the experimental data. Because B diffusion occurs during the heating of the samples (10 °C/min) from room temperature to the isothermal treatment temperatures as discussed earlier, there will be some pre-existing layer thickness that is not part of growth at the diffusion temperatures. Hence, this must be subtracted from the experimental data for a meaningful comparison with experiments. To determine the approximate amount of TiB_2/TiB layer growth during the heat-up period, samples were borided for 5 min at 850 °C, 950 °C and 1050 °C using the same heating rates. The layer thicknesses obtained in these experiments are given in Table 1.

3.3. Comparison with experimental data

For the present calculations, the B diffusion coefficients were determined from the work of Fan et al. [29] and are reported in Table 2. The TiB layer growth is accelerated due to the fast diffusion of B in [0 1 0], and therefore, the estimated B diffusivity in TiB is specific to this direction. The diffusivities of Ti in TiB_2 and TiB are 10^3 to 10^4 times lower than that of B in these phases [29–31]. Hence the effect of Ti diffusion on layer growth can be neglected.

Fig. 8 shows the predicted TiB_2 thickness development as a function of time, compared against the experimental data. The experimental data have been corrected for the 5 min growths—the TiB_2 thicknesses, observed after 5 min at the respective temperatures, were deducted from the original thicknesses. A reasonable agreement between the predicted data and the experimental data at 850 °C and 1050 °C can be seen. In most cases, the predicted layer thicknesses of TiB_2 are within 10–20% of the experimental data. But the numerical predictions at 950 °C are slightly higher than the experimental trend. Especially for treatment times exceeding 6 h, the numerical predictions are 20–30% higher than the experimental values. Based on our recent research [23], it was also found that the TiB_2 layer recedes due to a complex mechanism involving enhanced anomalous diffusion in Ti near the α/β phase transition temperature. The temperature region for such anomalous diffusion in Ti can extend up to 950 °C [32]. It is therefore suggested that the small difference (20–30%) between the predicted and the experimental TiB_2 layer thickness at

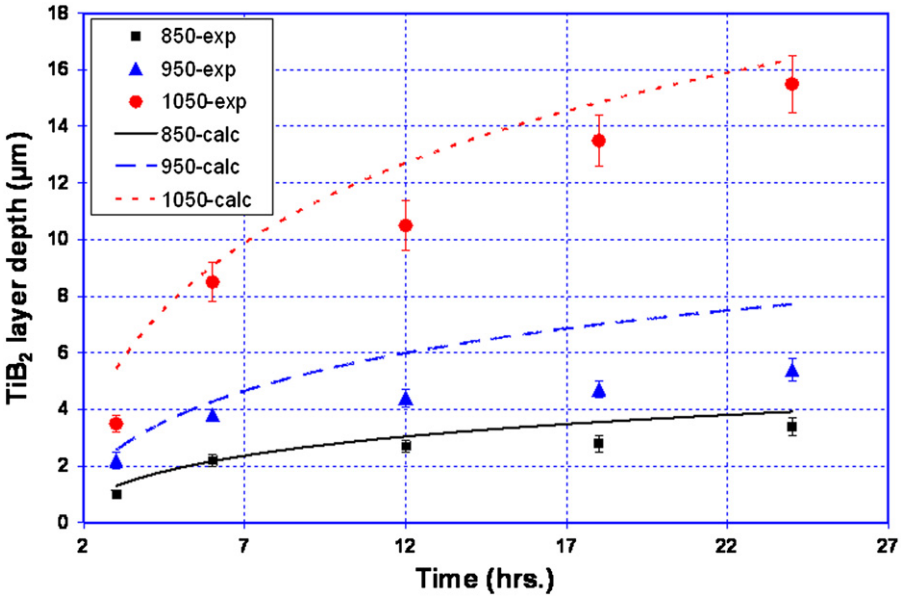

Fig. 8. Comparison of the predicted and the experimentally measured TiB_2 thicknesses, after correcting for the TiB_2 layer growth due to 5 min exposure.

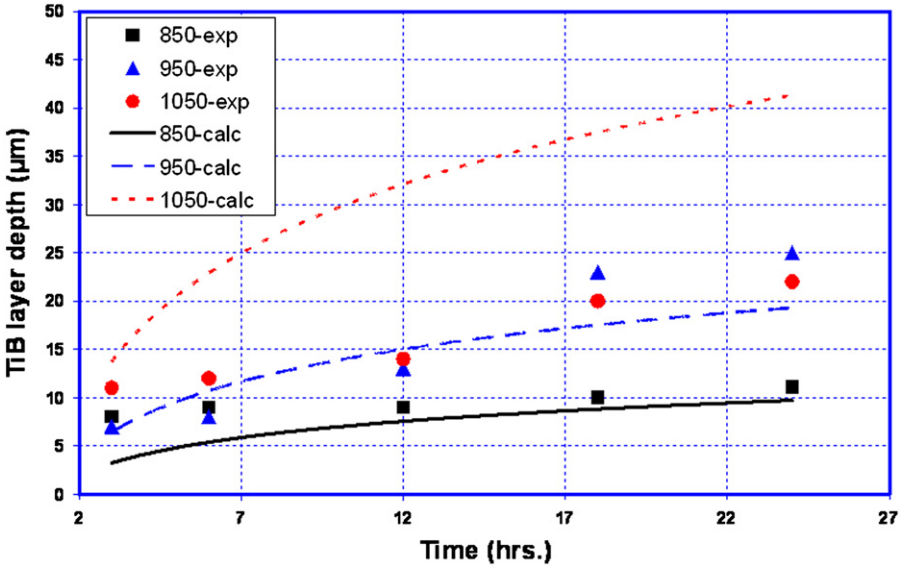

Fig. 9. Comparison of the predicted and the experimentally measured TiB coating layer thicknesses, after correcting for the TiB layer growth due to 5 min exposure.

950 °C, especially at longer boriding times, is due to the TiB_2 layer recession. This effect is absent at 850 °C and 1050 °C and this might explain the agreement of the experimental and the predicted data at these temperatures. It is also to be noted here that the reasonable agreement between the predicted and experimental values of TiB_2 layer thicknesses also negates any argument of oxidation during boriding. If the TiO_2 layer were to have formed and retarded the growth kinetics of the boride layers, the experimental TiB_2 layer thicknesses would have been much lower than the theoretically predicted values at all boriding temperatures. Hence, it appears to be reasonable to conclude that oxidation did not affect boride layer growth kinetics significantly.

Fig. 9 is the comparison of the experimentally measured TiB coating thicknesses (after deducting the TiB thicknesses due to 5 min exposure) and the predicted growth data. The predictions are in reasonable agreement with the experimental data at 850 °C and 950 °C. Most of the numerically data are in the range of 20–25% of that of the experimental values. However, there is a large discrepancy between the predicted and the experimental data at 1050 °C by about a factor of two. Actually, the experimental growth data at 1050 °C, being nearly similar to that at 950 °C, is itself quite unusual. This may be attributed to the thickening of TiB whiskers at high temperatures. While almost all of the TiB whiskers were

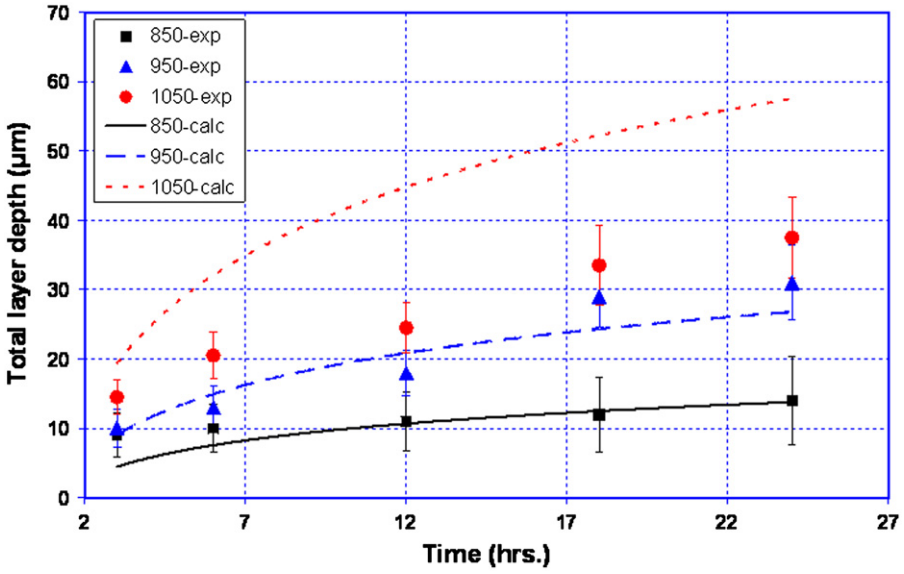

Fig. 10. Comparison of the predicted and the experimentally measured total (TiB_2+TiB) coating layer thicknesses, after correcting for the TiB_2 and the TiB layer growth due to 5 min exposure.

relatively thin at 850 °C and 950 °C; at 1050 °C, many TiB whiskers in the layer were relatively thicker (Fig. 3). It was suggested earlier [33] that diffusion in the transverse direction of TiB whiskers is about 10 times slower than that in the [0 1 0] direction, which is the axial direction of whiskers. This means that the rates of thickening and lengthening will be about equal, when the whisker aspect ratio reaches 10. Above this aspect ratio, thickening of TiB whiskers provides a faster means of transporting B and reacting with Ti, as opposed to the axial transport and extension of growth along the TiB axial direction. Since the model predictions are based only on diffusivities for growth along the [0 1 0] TiB direction, they should not agree with the experimental data of total layer thickness at 1050 °C, if TiB whiskers appear to be much thicker than those at lower temperatures. Fig. 3(a and b) indicate that this may be the case—a significant fraction of TiB is no longer whiskers and they appear to thicken due to increased B diffusion in the direction transverse to TiB whisker axis. Further study of TiB thickening will be performed in the future.

Fig. 10 shows the comparison of the total (TiB_2+TiB) layer thickness predictions with the experimental data. The predictions for the 850 °C and 950 °C are in reasonable agreement with the experimental data, while at 1050 °C; the predicted thicknesses are relatively higher. This difference arises from the TiB layer growth behavior as discussed above.

4. Conclusions

1. Superhard, dual boride layers consisting of a monolithic TiB_2 layer, followed by a TiB whisker layer are formed, with the TiB whiskers penetrating normally into the titanium surface during solid state diffusion of B.
2. The thickness of the TiB_2 layer increases with time and temperature with a relatively higher TiB_2 layer thicknesses resulting at diffusion temperatures in the β-phase field.
3. The growth rate and the maximum layer thickness attained for the TiB whisker layer seem to reach a maximum at 950 °C, which is the closest to the β-transus temperature (913 °C) of all the temperatures studied.
4. X-ray diffraction analysis confirmed the presence of both TiB_2 and TiB layers in all samples irrespective of the boring time and temperature.
5. The total layer thickness is actually dominated by TiB whiskers at temperatures 850 °C and 950 °C, whereas at 1050 °C, the TiB_2 layer becomes a significant fraction of the total layer thickness. This difference is attributed to the diffusivities of B in TiB–B transport in the TiB axial direction seems to be reduced when the TiB whiskers grow too long and this seems to lead to accumulation of B in TiB_2, resulting thicker TiB_2 layer at high temperature.
6. The growth of TiB_2 as well as that of total (TiB_2+TiB) layer was found to obey the parabolic kinetics. Error function solutions were developed based on Fick's second law to predict boride layers growth kinetics. A reasonable agreement between the predictions of these solutions with the experimental data was found in most cases with the exception of when TiB whiskers begin to thicken.

Acknowledgements

The authors acknowledge the support of this research by the Office of Economic Development of the State of Utah

through the Center of Excellence Program as well as by Ortho Development Corporation, Draper, UT.

References

[1] E. Metin, O.T. Inal, Kinetics of layer growth and multiphase diffusion in ion-nitrided titanium, Metallurgical Transactions A 20A (9) (1989) 1819.

[2] T.M. Muraleedharan, E.I. Meletis, Surface modification of pure titanium and Ti–6Al–4V by intensified plasma ion nitriding, Thin Solid Films 221 (1–2) (1992) 104.

[3] C. Boettcher, First prize deep case hardening of titanium alloys with oxygen, Surface Engineering (UK) 16 (2) (2000) 148.

[4] R.A. Poggie, P. Kovacs, J.A. Davidson, Oxygen diffusion hardening of Ti–Nb–Zr alloy, Materials and Manufacturing Processes 11 (2) (1996) 185.

[5] A. Bloyce, P.H. Morton, T. Bell, Surface engineering, ASM Handbook 5 (1994) 835.

[6] Y. Itoh, A. Itoh, H. Azuma, T. Hioki, Improving the tribological properties of Ti–6Al–4V alloy by nitrogen-ion implantation, Surface and Coatings Technology 111 (1999) 172.

[7] L. Liu, F. Ernst, G. Michal, A. Heuer, Surface hardening of Ti alloys by gas-phase nitridation: kinetic control of the nitrogen surface activity, Metallurgical and Materials Transactions 36A (2005) 2429.

[8] E. Rolinski, Surface properties of plasma-nitride titanium alloys, Material Science & Engineering. A108 (1989) 37.

[9] D. Nolan, S. Huang, V. Leskovsek, S. Braun, Sliding wear of titanium nitride thin films deposited on Ti–6Al–4V alloy by PVD and plasma nitriding processes, Surface and Coatings Technology 200 (2006) 5698.

[10] J. Satoh, Y. Shibuya, M. Satoh, et al, The new surface modification method of titanium, International Conference on Functionally Graded Materials Technology Leveraged Applications, Denver, Colorado, Metal Powder Industries Federation, (2002), 123–136.

[11] H. Dong, X. Li, Oxygen boost diffusion for the deep-case hardening of titanium alloys, Material Science & Engineering A280 (2000) 303.

[12] E. Atar, E.S. Kayali, H. Cimenoglu, Characteristics and wear performance of borided Ti6Al4V alloy, Surface and Coatings Technology 202 (2008) 4583.

[13] H. Krzyminski, H. Kunst, Treatment of refractory metals. I: Method technology II: constitution and characteristics of the boride layers, HTM 28 (2) (1973) 100.

[14] S. Aich, K.S. Ravi Chandran, TiB whisker coating on titanium surfaces by solid-state diffusion: synthesis, microstructure, and mechanical properties, Metallurgical and Materials Transactions A: Physical Metallurgy and Materials Science 33 (11) (2002) 3489.

[15] N. Tikekar, K.S. Ravi Chandran, A. Sanders, Novel double-layered titanium boride coatings on titanium: kinetics of boron diffusion and coating morphologies, TMS Letters (3) (2005) 87.

[16] N. Tikekar, K.S. Ravi Chandran, A. Sanders, Nature of growth of dual titanium boride layers with nanostructured TiB whiskers on the surface of titanium, Scripta Materialia 57 (3) (2007) 273.

[17] C. Lee, A. Sanders, N. Tikekar, K.S. Ravi Chandran, Tribology of titanium boride-coated titanium balls against alumina ceramics: wear, friction , and micromechanisms, Wear 265 (2008) 375.

[18] A.P. Sanders, N. Tikekar, C. Lee, K.S. Ravi Chandran, Surface hardening of titanium articles with titanium boride layers and its effects on substrate shape and surface texture, Journal of Manufacturing Science and Engineering 131 (3) (2009) 031001 1.

[19] R. Chatterjee-Fischer, O. Schaaber, Boriding of steel and non-ferrous metals, Proceedings of the 16th International Heat Treatment Conference, Stratford-upon-Avon, (1976).

[20] S.C. Singal, An erosion-resistant coating for titanium and its alloys, Thin Solid Films 53 (1978) 375.

[21] H. Celikkan, M.K. Ozturk, H. Aydin, M.L. Aksu, Boriding titanium alloys at lower temperatures using electrochemical methods, Thin Solid Films 515 (2007) 5348.

[22] B. Sarma, K.S. Ravi Chandan, Accelerated kinetics of surface hardening by diffusion near phase transition temperature: mechanism of growth of boride layers on titanium, Acta Materialia 59 (2011) 4216.

[23] W. Jost, Diffusion in Solids, Liquids Gases, Academic Press Inc, New York, 1960 6972.

[24] J. Crank, The Mathematics of Diffusion, Clarendon, Oxford, 1975.

[25] C. Brakman, A.W.J. Gommers, E.J. Mittemeijer, Boriding of Fe and Fe–C, Fe–Cr, and Fe–Ni alloys; boride-layer growth kinetics, Journal of Matematik Research 4 (1989) 1354.

[26] L. Yu, X. Chen, K. Khor, G. Sundararajan, FeB/Fe_2B phase transformation during SPS pack-boriding: boride layer growth kinetics, Acta Materialia 53 (2005) 2361.

[27] M. Keddam, S. Chentouf, A diffusion model for describing the bilayer growth (FeB/Fe_2B) during the iron powder-pack boriding, Applied Surface Science 252 (2005) 393.

[28] Z. Fan, Z.X. Guo, B. Cantor, The kinetics and mechanism of interfacial reaction in sigma fibre-reinforced Ti MMCs, Composites—Part A: Applied Science and Manufacturing 28 (2) (1997) 131.

[29] J.L. Murray, P.K. Liao, K.E. Spear, The B–Ti (boron–titanium) system, Bulletin of Alloy Phase Diagrams 7 (6) (1986) 550.

[30] H. Schmidt, G. Borchardt, C. Schmalzried, R. Telle, S. Weber, H Scherrer, Self-diffusion of boron in TiB_2, Journal of Applied Physics 93 (2003) 907.

[31] J.M. Sanchez, D.DE. Fontaine, Anomalous diffusion in omega forming systems, Acta Metallurgica 26 (1978) 1083.

[32] S.S. Sahay, K.S. Ravichandran, R. Atri, B. Chen, J. Rubin, Evolution of microstructure and phases in in-situ processed Ti–TiB composites containing high volume fractions of TiB whiskers, Journal of Materials Research 14 (1999) 4214.

[33] A.O. Prytula, I.N. Pogrelyuk, V.N. Fedirko, Effect of impregnating atmosphere oxygen on boriding of titanium alloys, Metal Science and Heat Treatment 50 (5) (2008) 232.